Design and Analysis of Single Mode Single Polarization Photonic Crystal Fiber

A Dissertation submitted towards the partial fulfillment of the requirement for the award of degree of

Master of Technology in
Microwave and Optical Communication Engineering

Submitted by
Naik Kishor Dinkar
2K13/MOC/06

Under the supervision of
Dr. Ajeet Kumar
Assistant Professor

Department of Applied Physics and Department of Electronics & Communication Engineering

Delhi Technological University
(Formerly Delhi College of Engineering)

JUNE 2015

DELHI TECHNOLOGICAL UNIVERSITY

Established by Govt. Of Delhi vide Act 6 of 2009

(Formerly Delhi College of Engineering)

SHAHBAD DAULATPUR, BAWANA ROAD, DELHI-110042

CERTIFICATE

This is to certify that work which is being presented in the dissertation entitled

"Design and Analysis of Single Mode Single Polarization Photonic Crystal Fiber" is the authentic work of **Naik Kishor Dinkar** under my guidance and supervision in the partial fulfillment of requirement towards the degree of **Master of Technology in Microwave and Optical Communication Engineering**, jointly run by Department of Applied Physics and Department of Electronics & Communication Engineering in Delhi Technological University during the year 2013-2015.

As per the candidate declaration this work has not been submitted elsewhere for the award of any other degree.

Dr. Ajeet Kumar
Supervisor, Assistant Professor
Department of Applied Physics

DECLARATION

I hereby declare that all the information in this document has been obtained and presented in accordance with academic rules and ethical conduct. This report is my own, unaided work. I have fully cited and referenced all material and results that are not original to this work. It is being submitted for the degree of Master of Technology in Microwave and Optical Communication Engineering at Delhi Technological University. It has not been submitted for any degree or examination in any other university.

Naik Kishor Dinkar
M. Tech. MOCE
2K13/MOC/06

ABSTARCT

Photonic Crystal fibers consisting of defect region at a center surrounded by multiple air holes running along its length have been the topic of most interest of researchers because of unique properties over conventional optical fibers. Here basics of Photonic Crystal Fibers, PCFs modeling methods are discussed.

A rectangular core photonic crystal fiber structure has been designed based on higher order mode filtering, in which single polarization is obtained with asymmetric design and introducing different loss for x-polarization and y-polarization of fundamental mode. Single polarization single mode operation of a highly birefringent photonic crystal fiber is investigated in detail by using a full vector finite element method with anisotropic perfectly matched layer.

The variations of confinement loss and effective mode area of x-polarization and y-polarization of fundamental mode have been simulated by varying the structural parameters of the proposed photonic crystal fiber. At optimized parameters, the confinement loss and effective mode area is obtained as 0.94 dB/m and 60.67 μm^2 for x-polarization as well as 26.67 dB/m and 67.23 μm^2 for y-polarization of fundamental mode respectively at 1.55 μm. Therefore, 0.75 m length of fiber will be sufficient to get x-polarized fundamental mode with effective mode area as large as 60.67 μm^2.

Key words: Photonic Crystal Fiber, Single Mode, Single Polarization, High Birefringent, Finite Element Method, Comsol Muliphysics, Effective Refractive index, Confinement Loss, Effective Mode Area

LIST OF RESEARCH PRESENTATION AND PUBLICATIONS

1. Ajeet Kumar, Than Singh Saini, **Kishor D. Naik**, Ravindra K. Sinha, "Design and analysis of rectangular-core large-mode-area photonic crystal fiber," Proc. International Conference on Recent cognizance in wireless communication & image processing (ICRCWIP-2015), 16 – 17 January 2015, pp.46, Poornima Institute of Engineering & Technology, Jaipur, INDIA.

2. **Kishor D. Naik**, Than Singh Saini, Ajeet Kumar, Ravindra K. Sinha, "Design of single mode single polarization large mode area photonic crystal fiber," Proc. SPIE-Optics & Photonics: Advances in Photonic Crystals and Materials II, 9 – 13 August 2015, San Diego, USA (Accepted for oral presentation) paper number: 9586-15

ACKNOWLEDGEMENT

I take this opportunity as a privilege to thank all individuals without whose support and guidance, I could not have completed my project successfully in this stipulated period of time.

First and foremost I would like to express my deepest gratitude to my supervisor **Dr. Ajeet Kumar**, Asst. Professor, Department of Applied Physics, for his invaluable support, patient guidance, motivation and encouragement throughout the period this work was carried out. I would also like to thank **Than Singh Saini**, Research Scholar, for valuable time and interest in this project. I am grateful to both for closely monitoring my progress and providing me with timely and important advice, their valued suggestions and inputs during the course of the project work.

I am deeply grateful to **Prof. S. C. Sharma**, H.O.D. (Deptt. Of A.P.), **Prof. Prem R. Chadha,** H.O.D. (Deptt. Of E.C.E), **Prof. R. K. Sinha,** and **Prof. Rajiv Kapoor** for their support for providing best educational facilities.

I also wish to express my heart full thanks to the classmates as well as staff at Department of Applied Physics and Department of Electronics & Communication of Delhi Technological University for their goodwill and support that helped me a lot in successful completion of this project.

Finally, I want to thank my parents, brother and friends for always believing in my abilities and for always showering their invaluable love and support.

Naik Kishor Dinkar
M. Tech. MOCE
2K13/MOC/06

CONTENTS

List of Tables

List of Figures

Chapter 1

Introduction

1.1 Thesis Approach:

This thesis consists of a design of rectangular-core photonic crystal fiber which supports single-mode and single-polarization. Single-polarization means light of specific polarization is only allowed to propagate through the fiber and is obtained by high-birefringence between two polarizations of fundamental mode propagating through the fiber. Single-mode is obtained with high confinement loss difference between two polarizations of fundamental mode as well as fundamental mode and all higher order modes. The rectangular-core single-mode single-polarization photonic crystal fiber design is put forward and analyzed in 'Comsol-Multiphysics' software, which solves complex electromagnetic fields using Finite-Element Method. Using Finite-Element Method effective-refractive-index, confinement-loss, and effective-mode-area for x-polarization and y-polarization for fundamental mode is calculated. And the effects of various structural parameters and spectral bandwidth are also investigated.

1.2 Thesis Objectives:

The main objectives of the thesis are given as follows:

- Study of the basic properties of photonic crystal fiber such as single-mode operation, birefringence, confinement losses, and effective-mode-area.
- Study the basics of various modeling methods which are used to model photonic crystal fibers, like Effective-Index Approach, Plane-Wave-Expansion Method, Finite-Difference Time-Domain Method, and Finite-Element Method.
- Design and analysis of rectangular-core single-mode single-polarization photonic crystal fiber based on asymmetric design.
- Study the effect of structural parameters and spectral band on effective-refractive-index, confinement loss, and effective-mode-area of x-polarization and y-polarization of fundamental mode.

1.3 Thesis Organization:

The outcome of the work carried out in this project is organized in five chapters. Chapter 1 consists of an introduction and objectives of the thesis. A literature review of the topic of project, basics of photonic crystal fibers, its properties, as well as its various applications in novel fields are explained in chapter 2. Chapter 3 gives the idea about modeling methods of the photonic crystal fiber. Chapter 4 is related with design and analysis of rectangular-core single-mode single-polarization photonic crystal fiber. The rectangular-core design is proposed for single-mode and single-polarization operation. In chapter 5, the work carried out is concluded with suggestions for future work that can be done in this field.

Chapter 2

Photonic Crystal Fibers

2.1 Introduction:

In the last few years, Optical fiber communication system is dominating the other communication systems like analog, digital, wireless etc. because of its advantages like high bandwidth, low transmission losses, high signal security, low electromagnetic/ radio frequency interference, low cost per bandwidth, low maintenance and so on [1]. Optical fibers have attracted more attention of the researchers because it is very important elements in the optical fiber communication systems. The guidance of light through optical fiber is based on two different doping levels (refractive-indices), core and cladding. Central region i.e. core is made up of slightly higher refractive-index material than cladding this difference is measured as numerical aperture. Because of the difference in refractive-index of core and cladding, the light guides inside the core by the phenomenon called Total-Internal-Reflection (TIR) or in some cases Photonic-Band-Gap (PBG). The various types of optical fibers are developed such as step-index fibers, graded-index fibers. These fibers can be single-mode or multi-mode depending on the dimension of the core and cladding of the fibers [2]. Optical fibers are selected for intended application on basis of a careful selection off optical losses, optical non-linearity, polarization effects, and group velocity dispersion (GVD). Non-linearity, losses, polarization and GVD are directly related to the raw material used to make the fibers, Silica and silicon dioxide. Non-linearity and chromatic dispersion are decided by the material properties, where as polarization and losess by imperfections in fabrication process of fibers. Non-linearity, losses, Polarization effects and GVD are also influenced by design of optical fiber.

Conventional optical fiber technology is limited due to necessity of very small and highly controlled refractive-index steps between core and cladding and also its dimensions plays very important role. Photonic crystal fibers (PCF) eliminate limitations of conventional optical fibers. With appropriate materials and precise dimensions PCFs can give a massive range of effective-indices thus highly linear or highly non-linear fibers are developed and used. Furthermore, PCFs are developed to manage low losses, polarization and chromatic dispersion by properly tailoring various parameters. PCF technology's inventor Prof. Philip Russell told that PCFs mark the start of a new age in optical fiber communications. [3-4]. On

the other hand, PCFs enabled light to be guided and controlled in such a ways that no one thought previously possible or even imaginable. First PCF designed and fabricated by Prof. Jonathan Knight in 1995 [5-6].

Variation of refractive-index leads to guidance of light in PCFs and enclosed light within small and periodic air-holes which forms cladding region. This characteristic makes the cladding index to strongly depend on wavelength. Shorter wavelengths stay tightly restricted within the core because the cladding index is slightly inferior to the core index. At longer wavelengths, the mode spreads in cladding, high effective-index contrast. This wavelength dependence is unusual and which indicates that optical properties can be tailored in controlled manner. PCFs are also known as microstructured fibers as wavelength scaled, periodic, minute structure i.e. micro structures running throughout its length. PCFs are making progress day by day in terms of fiber structures, fiber materials, fiber fabrication methods etc. , these advantages over regular conventional fiber technology enables a large range of fascinating applications [7-10].

2.2 Guidance mechanisms in PCF:

Light guidance in PCFs is based on fact of TIR or PBG, which has contingent on the core and cladding materials. Pure silica, doped silica, or highly non-linear glasses are used to form core of PCFs whereas array of air-holes or other material rods with material same as core builds cladding of PCFs. The PCFs are divided in four categories as follows, taking into consideration of propagation mechanism in PCFs behind the guidance of the light.

2.2.1 Index-Guiding PCFs:

One of the simplest types of fiber is Index-Guiding Photonic Crystal Fibers (IG PCFs) since light guidance is based on modified TIR. IG PCF has a solid core made up of pure silica, with tiny distinct array of air-holes, set in hexagonal, rectangular, triangular, circular, or spiral pattern. This core of IG PCF is solid, basically formed by introducing defects in the geometry of PCF. The refractive-index profile and the diagram of this type of PCF is shown in Fig 2.1 (a).

The solid core has same material as the PCF cladding, which states that refractive-index of core is superior to the refractive-index of cladding region due to microstructured array of air-holes. The defect at the center of the core of PCF structure is realized by removal of the

central capillary or many capillaries around central. The Electromagnetic wave i.e. light is guided in PCF can be considered as a modified TIR mechanism. The network of air-hole capillaries leaks higher order modes which then gives confinement to fundamental mode. This modification gives the mode which has smallest diameter, this diameter is closed to the defect size at center [4, 5].

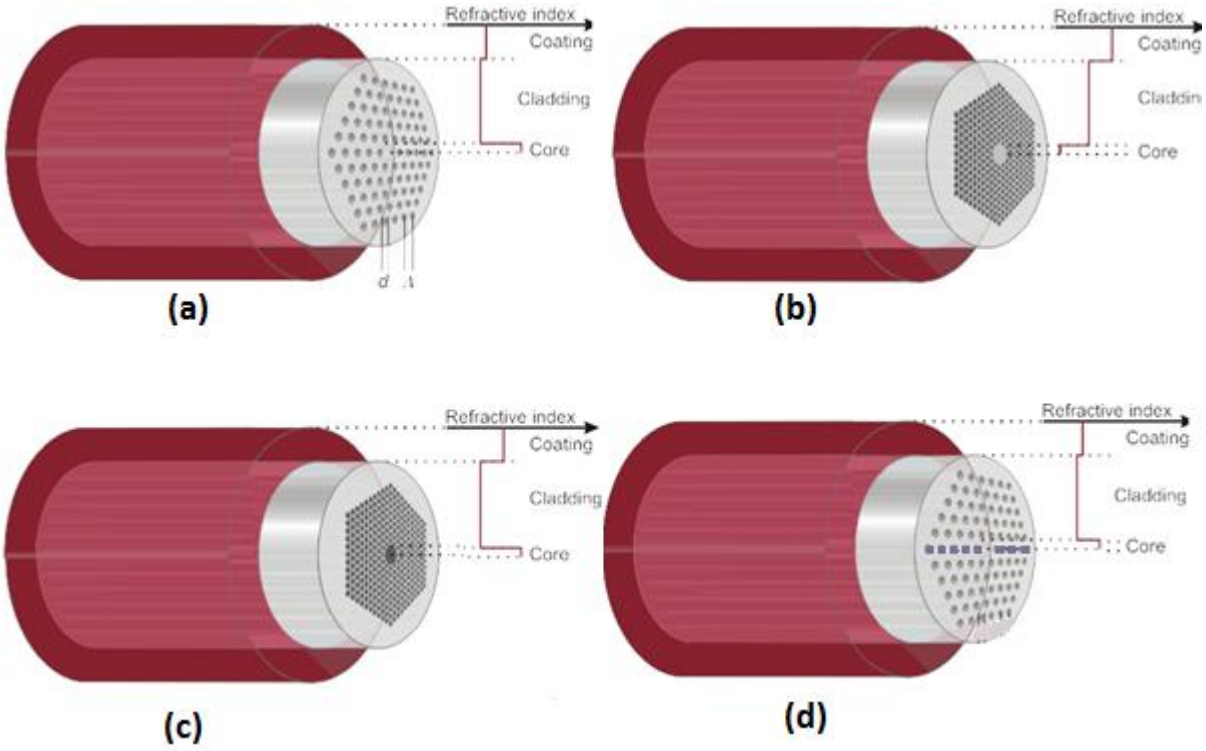

Fig. 2.1 Photonic crystal fiber: (a) Index Guiding PCF, (b) Hollow Core PCF, (c) Photonic Band Gap PCF (All Photonic Bandgap Fiber) and (d) Hybrid PCF (Source: NKT Photonics website)

The main design parameters in PCFs are the air-hole diameter (d)/ radius (r), hole-to-hole spacing i.e. pitch (∧), and air-holes layer numbers. The PCFs are generally narrated by the air-filling fraction. Thus air-filling fraction can be given as ratio of the air hole diameter inside cladding to pitch in PCF. So we can easily manipulate the air-filling fraction to change the propagation constant of guided modes, non-linear properties, and dispersion on the basis of required applications of PCFs [3-10].

2.2.2 Hollow-Core PCFs:

In Hollow-Core (HC) PCFs, Guidance of the light is based on external-reflection. IG PCF has a HC made up by removal of capillaries from center region of PCF, with tiny distinct array of air-holes, set in hexagonal, rectangular, triangular, circular, or spiral pattern. The refractive-index profile and the diagram of this type of PCF is shown in Fig. 2.1(b) [8, 11].

HC PCFs gives quasi-single-mode operation by guidance of light trough HC made up of air, surrounded by cladding formed by air-holes in silica. HC PCFs hold numbers of optical-modes at any specified wavelength within the bandgap, Optical-modes include both air guided modes and surface modes. Careful designing and light launching gives the fundamental mode which is well confined through PCFs and also gives higher order modes but the higher order modes have more confinement loss and scattering loss as compared to the fundamental mode [12,13].

2.2.3 Photonic-Band-Gap PCF (All-Solid-Photonic-Band-Gap Fiber):

All-solid-photonic-bandgap fibers (PBGFs) are analogous to HC PCFs because many properties of PBGFs are present in HC PCFs. Photonic-band-gap guidance can also be experiential with solid core. In this type of fibers, the fiber bandgap is produced by an arrangement of high-index solid insertion. The PBGFs have high-index contrast if pure silica core is bounded by an array of germanium-doped silica rods. The PBGFs basically consist of unconnected high-index rods in the background of in a low-index material. The PBGFs guide the light of restricted bands of wavelength. In the PBGFs, the high-index rods in the cladding allow light to its leakage from the core at resonance, on the contrary they also reflect light back into the core at anti resonance. Each high index inclusion of the structure is considered as a waveguide that supports normal modes, along with their associated modal cutoff conditions. The stop-bands and pass-bands of spectral band are influenced by the arrangement of germanium-doped rods. The numbers of germanium doped rod layers are increased then it causes the decrement in the confinement. The typical PBGF structure is shown in Fig.2.1(c) [14, 15].

2.2.4 Hybrid PCFs:

This is one of the complex types of PCFs, hybrid (H) PCF is made up of germanium-doped silica and air-holes around pure silica core, The typical diagram and refractive-index profile

is shown in Fig.2.1(d). The air-hole are placed in hexagonal, square, rectangular, and/or spiral pattern as in the IG PCFs, apart from it, germanium-doped silica rods which is having the high-index are replaced a single row of air-hole along one of the axes of PCF, forming a one-dimensional PBG in this direction.

Suppose H PCFs have germanium-doped silica roads along x-axis, thus along x-axis core has lower effective-refractive-index as compare to cladding then TIR is not possible whereas along y-axis effective-refractive-index of core is higher than cladding so TIR is permitted thus guidance of light [16].

2.3 Properties of PCFs

2.3.1 Single-Mode Fiber:

For various applications single-mode PCFs are favored in a large range wavelength in visual and near infrared band. Classical optical fibers (step-index fibers) have its cut off frequency. The cut off frequency is the frequency over which fibers support multi-mode. A normalized frequency is useful in determination of the number of guided modes in step-index fibers. Normalized frequency (V) usually defined as the relation

$$V = \frac{2\pi r}{\lambda}\sqrt{({n_{core}}^2 - {n_{cladding}}^2)} \qquad (2.1)$$

where, r: core radius, n_{core} : refractive-index of the core and $n_{cladding}$: refractive-index of the the cladding. Refractive-index of core is depending upon wavelength while refractive-index of cladding is wavelength independent. From Eq. 2.1, we can say normalized frequency is inversely proportional to wavelength which means that, if wavelength increases V number decreases, hence number of modes decreases. Conventional optical fibers result in multi-mode operation regime for normalized cut off frequency higher than 2.4051 [1, 2].

For PCF a value of the effective-refractive-index of cladding strongly rely on wavelength, in case of classical fibers it is almost constant. In case of PCFs, it is said to be single-mode when air-filling fraction is less than 0.4. Air-filling fraction is given as the ratio of air-hole diameter to the period of lattice structure. Thus we get lot of freedom to design and obtained endlessly single-mode fibers over wide spectral range. The normalized frequencies have a tendency to be stationary value for short wavelengths. A refractive-index of cladding and stationary value of normalized frequency is distinct by the cladding structure, namely by the

air-filling factor. With a suitable design it is possible to keep normalized frequency below a cutoff for any wavelength range [18, 19, 22-26].

2.3.2 Large-Mode-Area:

Conventional optical fibers have restrictions on core size and numerical aperture (NA) for single-mode operation. The value of numerical apertures is proscribed by the difference in refractive-index of the core and the refractive-index of cladding. NA is given by Eq. 2.2.

$$\mathrm{NA} = \sqrt{({n_{core}}^2 - {n_{cladding}}^2)} \qquad (2.2)$$

For particular core diameter and wavelength, there is a maximum numerical aperture value which creates a single-mode regime of operation possible for fiber. The fabrication of a standard step index fiber also affects the single-mode operation and a large-mode-area [1, 2]. Thus we would require highly accurate refractive-index controlling fabrication method. Chemical vapor deposition is one of the methods which has a very high accuracy. The numerical apertures limit the mode-field-diameter (MFD). Usually the MFD of conventional step-index fiber is defined as $1/e^{th}$ of the maximum intensity, and for conventional optical fiber is about 9 µm for 1.55 µm wavelength. The MFD and effective-mode-area for conventional fiber is given in Eq. 2.4, and Eq. 2.5.

$$\mathrm{w} = \mathrm{r} \times \left(0.65 + \frac{1.619}{\mathrm{V}^{3/2}} + \frac{2.879}{\mathrm{V}^{6}}\right) \qquad (2.3)$$

$$\mathrm{MFD} = 2 \times \mathrm{w} \qquad (2.4)$$

$$\mathrm{A_{eff}} = \pi \times \mathrm{w}^2 \qquad (2.5)$$

where w: spot size, r: core radius, V: normalized frequency and $\mathrm{A_{eff}}$: effective-mode-area. In case of photonic crystal fiber large-mode-areas can be obtained by increasing the pitch of the photonic cladding or decreasing the air-hole diameter/radius or increasing the size of the defect in photonic cladding i.e. removal of few central air-holes. As shown by Baggett et al., [19] large core step-index fiber and PCF can have a same value for MFD at any given wavelength with a single capillary defect in case of PCF.

2.3.3 Birefringence:

For the polarization sensitive applications the birefringence plays an important role. Birefringence is stated as the difference between effective-refractive-indices of two polarizations of fundamental modes and is given as Eq. 2.6. Birefringence is also measured as beat length, L_B as shown in Eq.2.7.

$$B = n_x - n_y \tag{2.6}$$

$$L_B = \frac{2\pi}{\beta_x - \beta_y} = \frac{\lambda}{B} \tag{2.7}$$

where n_x , β_x: effective-refractive-index, propagation constant along x-axis respectively and n_y , β_y: effective-refractive-index and propagation constant along y-axis for mode respectively.

Photonic crystal fibers are made highly birefringent, introducing large index contrast between two polarizations. This can be accomplished introducing elliptical air-holes in cladding or asymmetric core or asymmetrical air-hole distribution along the two axes of fibers [20].

2.3.4 Dispersion property:

In conventional optical fibers mainly two types of dispersions i.e. material and waveguide dispersion gives total dispersion. In PCF waveguide dispersion can be altered to very high or to very low depending upon the desired applications. Material dispersion is also tailored by synthetic photonic cladding with the occurrence of air-holes. Photonic crystal cladding properties changes especially over a narrow range of spectral band. Group velocity dispersion is one of the most key parameter that describes properties of fibers. Group velocity dispersion (GVD) is defined as follows

$$GVD = \frac{\lambda}{c}\frac{d^2 n_{eff}}{d\lambda^2} \tag{2.8}$$

where n_{eff} : effective-refractive-index, c: velocity of light in vacuum.

$$n_{eff} = \frac{\beta(\lambda, nm(\lambda))}{k0} \tag{2.9}$$

Thus dispersion characteristics can be varied and shaped due to the litheness of varying air-hole size and air-hole position in the cladding region in photonic crystal fiber. Zero dispersion can be possible by varying pitch and air-hole sizes in PCFs. In other applications a zero dispersion wavelength can be switched into the visible region of wavelength [20, 21].

2.4 Applications of PCFs

The photonic crystal fibers have the unique properties which cannot be achieved using conventional optical fibers. The main applications of the PCFs according to their properties are described as follows.

2.4.1 Endlessly Single-Mode PCFs

In introduction, we already have mentioned that with certain geometries we can obtain PCFs which support only one mode which do not matter the size of the core or the wavelength. Generally these types of fiber are called endlessly single-mode PCFs, and PCFs are fabricated usually with a solid core enclosed by air-holes in cladding. PCFs property is very interesting and can have various applications, in the field of single-mode fiber lasers of low power and amplifiers in optical fiber communications systems.

2.4.2 Large-Mode-Area PCFs

Large-mode-area is directly related with power levels associated with PCFs, Higher the mode area, higher the power carrying capacity of the fiber. The very large-mode-area enables high power levels without material damage and non-linear effects. These properties are very interesting and can have various applications, including high power single mode fiber lasers and amplifiers.

2.4.3 Dispersion Compensating PCFs

A very interesting and one of the most vital applications of photonic crystal fiber is as dispersion tailoring devices. In the past fibers which were installed were operating at 1.33 µm but now a day's fibers are design to operate 1.55 µm. The fibers have more dispersion at 1.55 µm as judge against 1.33 µm. The photonic crystal fiber can be available as dispersion compensation fiber in order to remove or reduce the dispersion. Generally, the length PCFs are restricted due to more dispersion in communication links. This is especially important for wavelength division multiplexing, where compensation must be done in a broad range.

2.4.4 Highly Non-linear PCFs

Photonic crystal fibers with small core size and very high index contrast between core and cladding of PCFs are highly non-linear. These types of PCFs find various applications such as supercontinuum generation (white light laser sources), parametric amplification and slow light generation.

2.4.5 Polarization Maintaining PCFs

Birefringence in optical fibers arises due to the fabrication defects or stresses generated in fabrication process. Birefringence changes the transmission characteristics of fiber. Birefringence can be introduced in PCFs by bending, thermal effect, and asymmetric design etc. Due to birefringence different optical axes are generated. When light propagate along these different axes with different speeds results in phase difference which leads to generate elliptically polarized light. This is known as polarization mode dispersion. Single mode and single polarization is easily achieved in PCFs thus they find applications in sensors gyroscopes and interferometers.

Chapter 3

PCF Modeling Methods

In design and analysis of photonic crystal fibers (PCFs), PCF modeling is very essential. Numerical simulations perform major role in the PCF designing as well as PCF modeling. Effective-index approach, basis-function-expansion approach, and numerical approach are numerical-modeling methods for PCFs and those making very good progress day by day. The fundamental PCF characteristics e.g. cut off wavelength, chromatic dispersion, modal birefringence, and various losses are numerically evaluated by using full-modal-vector model. There are various modeling methods of PCFs. So far, not only an approximate scalar model but also full-vector model is used in those modeling methods. An approximate-scalar model is a valuable tool to use and provides good qualitative information about fiber model but have limitation on accuracy. However, in order to get accurate PCF model, it is essential to use a full-vector model. Specifically, a complete-vector model is compulsory for predicting sensitive quantities such as chromatic dispersion and birefringence. Here we required to study and explore the significance of each method because selection of modeling tool can have an effect on computational time, mandatory computational resources, and limits of the methods.

3.1 Effective-Index Approach (Method):

The Fig. 3.1 shows a typical six fold rotational symmetric index-guiding PCF. Effective-index approach (EIA) is the first approach introduced for PCFs modeling. This approach is form on a very simple scalar-model using an effective-index of core and cladding.

In this approach/method, an effective-index is estimated for the periodic recurring air-holes and silica structure in the cladding region and replacing the cladding by a uniform medium with the estimated effective-index, which results a correspondent step-index fiber consisting of a core as well as a cladding region with different refractive-indices. Thus qualitative information about PCFs can be acquired using this simple approach/method and well reputable fiber theory [17, 18].

As the core is made up of silica, the refractive-index of core is equal to the refractive-index of pure silica, but the effective-refractive-index of cladding is concluded with the assist of propagation constant of fundamental mode, which is propagating through the sporadically recurring air-hole-silica structure without any defects at central region. The space filling

modes are propagating modes through PCF's cladding material. The propagation constant is wavelength dependent.

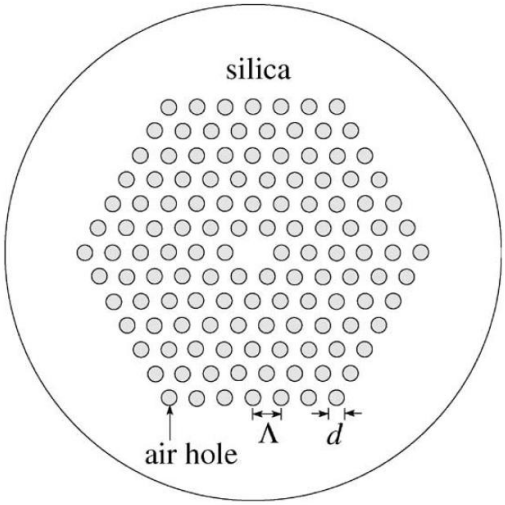

Fig. 3.1 Typical six fold rotational symmetric PCF (Source wiki)

The propagation constant, β available to light which is inside the core but is unavailable to light which is propagating in the cladding. $\beta_{FSM}<\beta<kn_{0,}$ where k : wave number, = $2\pi/\lambda$, n_0 : index of core, and β_{FSM} : propagation constant of the fundamental space filling mode (FSM).

3.2 Basis-Function-Expansion Approach:

In case of photonic crystal fibers, the EIA provides good quantitative information but not able to predict birefringence, dispersion, like modal properties. We know that dispersion and birefringence strongly depends on PCFs geometry. Full-vectorial methods are used to model PCFs. While modeling the PCFs various model putrefaction technique are using various basis functions such as sinusoidal, Hermite-Guassian,and Cylindrical functions etc.

3.2.1 The Plane-Wave-Expansion Method:

The Plane-wave-expansion method (PWEM) is one between most broadly used PCFs modeling method and applied for all type of PCFs, such as IG PCFs, PBGPCFs, HC PCFs [27-30]. PWEM is based on plane wave expansion of Electromagnetic fields, generally three components of magnetic fields. Electromagnetic fields are expanded using Bloch's theorem. Dielectric constant or position dependant permittivity is put across as a Fourier-series expansion.

A spatial defect in core region are replaced by supercells, spercell consists of periodically repeated spatial defects thus various properties of the defect region can be carried out very accurately. The supercells are large enough to calculate the properties of uncoupled defects. The modal fields and propagation constants are estimated by solving eigen value problem matrix. The eigen value matrix is based on minimization of plane wave equations and periodic boundary conditions.

3.2.2 The Localized-function Method:

The Localized-function method (LFM) is another approach in the basis-function-expansion method. Modal properties are well expressed by using LFM. Guided modes are localized in core region of PCFs thus modal fields are illustrated efficiently. To describe the modal fields localized Hermite-Gaussian functions are useful. Guided modes are model accurately with modest number of functions. This results in not as much of computational efforts, when compared with the PWEM. Electromagnetic fields (three components of the electric field) are decayed and index defects are converted to localized Hermite-Gaussian functions, and the lattice of air-holes with the help of sinusoidal functions. Avoiding use of many expansion terms each quantity is represented efficiently and accurately. These wave equations are reduced to eigen value problem matrix. The eigen value problem matrix gives modal field properties and their propagation constants [31, 32].

3.2.3 Multi-pole Method:

The modal fields are expanded in cylindrical harmonic functions because we generally have circular air holes in cladding region. Multipole Method (MM) is approach developing the local circular geometry. MM tells the leaky nature of PCFs with a limited number of air-holes. The two longitudinal-axis components of electromagnetic fields are distinct in terms of Bessel-Hankel functions. To define these functions local cylindrical coordinates are used. By using boundary conditions on surface of air holes, we can obtain all relations between the expansion coefficients [33-35].

3.3 Numerical Approach:

3.3.1 Beam-Propagation Method:

Beam-propagation method (BPM) is an approximation technique for simulation of photonic crystal fibers. The unusual structures of PCFs can be analyzed very accurately. The dynamic mode profiles are estimated significantly. The various mode properties can be found out using beam propagation method. Rigorous numerical simulations are difficult to carry when the wave is propagating along the waveguide for a large distance compared with wavelength. BPM depends on first order differential equation and can be solved as initial value problem. The spatial variables are involved in initial value problem rather than time. BPM is generally formulated as solution to the Hemholtz equations [36-38].

3.3.2 Finite-Difference Method and Finite-Difference-Time-Domain Method:

The finite-difference-time-domain method (FDTDM) is extensively used, and time domain numerical analysis method for modeling PCFs. FDTDM calculates the estimation of an electromagnetic field in depressive media of any properties over wide wavelength range [40-42]. FDTDM belongs to the class of grid based differential numerical modeling method. The time-dependent Maxwell's Equations are resolved using central-difference approximation of partial derivatives of space and time.

The FDTDM is very powerful and versatile which permits to obtain transmission and reflection coefficients, energy flow of propagation fields. The FDTDM also allows the inspection of a temporary field distribution as well as the steady state field distribution. The FDTD M is robust, universal, and methodologically simple as compared to others. High time consuming and memory complexity of the algorithm are main drawbacks of FDTDM.

3.3.3 Boundary-Element Method:

The two dimentional optical wavegude problems are solved using the Boundary Element Method (BEM). It has been shown that they are modeled with high accuracy and very precisely. Many PCFs are studied and analyzed using BEM. BEM require the integration along the boundary only. This indicates that meshing is mainly simple for two-dimensional problems. The solution of problem and its accuracy are affected by number of unknowns so, we can state that high accuracy is achieved with very few number of unknowns. External absorbing boundary conditions are not desired for open boundary is another different

advantage of BEM. In BEM encounters a non-standard eigen value problems for them direct search method is used. Direct search method requires finding the allocation of the determinant of the coefficient matrix. Coefficient matrix is nedded in order to obtain the wave number *k*. Due to this sometimes it becomes very time consuming [43, 44].

3.3.4 Finite-Element Method:

Unlike basis-function-expansion method, the wave equations are not solved, in Finite-Element-Method (FEM) while a full-vector mode solver formed on a hybrid-nodal FEM is used to decide the propagation constants as well as the electric field distributions of the guided modes. Which are solved with the help of the following generalized eigen value problem (GEP)

$$\begin{bmatrix} \nabla_T \times \nabla_T \times -k_0^2 n^2(r) & 0 \\ 0 & 0 \end{bmatrix} \begin{bmatrix} E_T \\ E_z \end{bmatrix} = -\beta^2 \begin{bmatrix} 1 & \nabla_T \\ \nabla_T & \Delta + k_0^2 n^2(r) \end{bmatrix} \begin{bmatrix} E_T \\ E_z \end{bmatrix} \quad (3.1)$$

The full-vector FEM has been applied to PCF modeling successfully [45, 46]. It permits calculating both dispersion and confinement properties of PBG and solid core structures. For a given wavelength the method gives a complex propagation constant

$$\gamma(\omega) = \beta(\omega) + i\alpha(\omega) \quad (3.2)$$

where β : standard propagation constant and α : attenuation constant.

Chapter 4

Rectangular-Core Single-Mode Single-Polarization Photonic Crystal Fibers

4.1 Introduction:

In recent years, Researchers are interested in Photonic crystal fibers (PCFs). PCFs have been attracting attention for their applications in field of optical fiber communication systems [5, 7, 17, 47]. PCFs have exclusive light guiding properties such as endlessly-single mode (SM) operation, dispersion tailoring, high birefringence (HB), large-mode-area (LMA), high non-linearity, and supercontinuum generation [48-56]. PCFs consist of a periodic array of air-holes in cladding around a central core of solid silica or air, the air-holes are running throughout its length. Various light guiding properties of the PCF are effectively controlled by manipulating the geometrical parameters such as lattice shape, air-hole shape, air-hole diameter or radius, and centre-to-centre distance of air-holes (*i.e.* pitch). Instead of air-holes many other material rods can be introduced.

Polarization-maintaining fibers (PMFs) which stabilize state of polarization are widely used in optical fiber communication systems and optical fiber sensor systems [57]. PMFs are made up of conventional HB fibers thus birefringence becomes one of the important characteristics of fibers. Conventional HB fibers are designed to operate in the single-mode single-polarization (SMSP). In SMSP PCFs, only one linearly polarized mode is guided and other orthogonal polarization mode is suppressed. It is difficult to get rid of the influence of polarization-mode-dispersion and polarization-mode-coupling on optical fiber communication system performance even with PMFs [58-60]. Now, HB PCFs have the ability to realize better SMSP. Because of that many SMSP fibers proposed which are based on HB PCFs. Conventional HB fibers have limitations on HB. PCFs have higher model birefringence due to the large index contrast and the stack-and-draw fabrication process. allow HB to be realized on PCFs. HB PCFs are made by designing with different sizes of air-holes i.e. radius/diameters along the both orthogonal axes or by designing asymmetric core of PCF or by modifying the shapes of air-holes near core of PCF and many more. As compare to conventional HB fibers, SMSP PCFs allows the propagation of one polarization state with elimination of the polarization-mode-coupling as well as polarization-mode-dispersion of fundamental mode [61-66].

Wideband SMSP propagation can be realized due to high index contrast. SMSP PCFs with a confinement-loss < 0.1 dB/km from 1.48-1.60 µm was proposed and analyzed in [67]. PCFs based on single-polarization fiber with a transmission loss of 28 dB/km and with a polarization dependent loss of 196 dB/km at 1.55 µm was reported in [68]. Numbers of designs were focused on SMSPs with LMAs that are useful in high power applications [69-71]. Low loss non-linear SMSP PCFs are utilized in optical fiber communication system applications, like wavelength conversion, wavelength multi-casting and parametric amplification [72]. Polarization dependent noises are eliminated by non-linear low loss SMSP PCFs and interaction efficiency is enhanced with the help of alignment of the polarization of the interacting electromagnetic waves in the same direction. Zero-dispersion or small slopes would yield applications such as polarized supercontinuum generation [73]. In [74] SMSP PCFs are designed at 1.33 and 1.55 µm, but these designed PCFs have the effective-mode-area below 40 μm^2.

In this paper, we have designed a rectangular-core (RC) SMSP PCF structure which gives effective SMSP operation with effective-mode-area (EMA) as large as 60.67 μm^2. By suppressing modes of higher order, single-mode operation has been achieved while by means of high differential confinement-loss between the two orthogonal polarizations of fundamental modes, high birefringence, single-polarization operation has been achieved. The PCF is designed in such a way that initially it supports both polarizations of fundamental mode, out of which only x-polarization of fundamental mode is perfectly guiding and y-polarization is leaky in nature. The effects of variation of geometrical parameters of PCF such as air-hole radius, pitch and effect of spectral band on the characteristics of SMSP operation are observed. A full-vector FEM with absorbing boundary conditions named as perfectly matched layers (PMLs) is used to evaluate the polarization dependent loss at 1.55 µm.

4.2 RC SMSP PCF Design

The transverse cross-sectional view of proposed RC SMSP PCF structure is presented in Fig.4.1 in which the six rectangular arrays of air-holes are drawn along the length of the fiber. In the proposed RC SMSP PCF structure, central air-hole has been detached to create the defect at core region as well as to create RC of the PCF.

As illustrated in Fig.4.1, there are two types of air-holes (having radius r_1 and r_2) arranged in four complete rectangular rings and two incomplete rectangular rings. The radius of smaller

air-holes is represented by r_1. Remaining all larger air-holes have radius r_2. The hole to hole distance (*i.e.* pitch) is taken as Λ. The birefringence can be enlarge by making design asymmetric, the asymmetric arrangement of the air-holes shown in rectangle gives the different effective refractive index characteristics to x and y-axis i.e x and y-polarization.

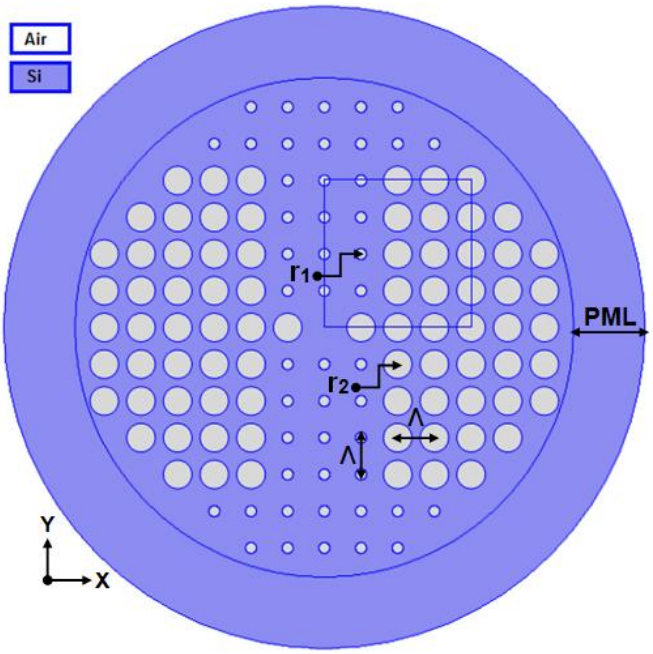

Fig.4.1: RC SMSP PCF.

4.3 Method of Analysis

To calculate the effective-index of fundamental mode travelling in the PCF, full vectorial FEM based software 'COMSOL' has been employed. To obtain wavelength dependent refractive index of the silicon, following Sellmeier equation has been used [75, 76].

$$n^2(\lambda) - 1 = \sum_{i=1}^{j} \frac{B_i \lambda^2}{\lambda^2 - {l_i}^2} \qquad (4.1)$$

Where, j = 3, B_1 = 0.6961663 , B_2 = 0.4079426, B_3 = 0.8974794, l_1 = 0.0684043, l_2 = 0.1162414, and l_3 = 9.896161 are Sellmeier coefficients and λ is the operating wavelength and $n(\lambda)$ is the wavelength dependent refractive index.

Software simulate solution of the following equation 4.2

$$\nabla \times ([s]^{-1} \nabla \times E) - k_0^2 n^2[s]E = 0 \qquad (4.2)$$

$$[s] = \begin{pmatrix} \frac{s_y}{s_x} & 0 & 0 \\ 0 & \frac{s_x}{s_y} & 0 \\ 0 & 0 & s_x s_y \end{pmatrix} \qquad (4.3)$$

where, E: Electric field, $\mathbf{k_0} = \frac{2\pi}{\lambda}$: Wave number in the vacuum, λ: Wavelength, n: Refractive-index, [s]: PML matrix, and s_x , s_y : PML parameters.

The propagation constants of modes turn to complex, when, we solve the Eq.4.2 for given PCF structure. The effective indices of modes are given by the real part of the propagation constant while the confinement losses of the modes are given by imaginary part of propagation constant. The following Eq. 4.4 gives the effective-refractive-index of the mode.

$$n_{eff} = Re\left(\frac{\beta}{k_0}\right) \qquad (4.4)$$

where, β: Propagation constant and it can be computed by solving eigen value equation. By reducing the index contrast or reducing the air hole sizes in PCFs the effective-mode-area of modes can be enhanced. On the other hand, reducing the index contrast there is an increment in confinement-loss of the modes which are traveling in the PCF.

Confinement loss can be computed using the imaginary part of effective-refractive-indices of modes by the following relation 4.5 [77].

$$CL\left(\frac{dB}{m}\right) = \frac{40\,\pi}{\ln(10)\lambda} Im(n_{eff}) = 8.686 k_0\, Im(n_{eff}) \qquad (4.5)$$

A circular PML is implemented at the fiber surface to simulate the effect of an infinite domain in the FEM. With the PML the propagation constant of modes becomes complex. The effective indices of modes are given by the real part of the propagation constant while the confinement losses (CL) of the modes are given by imaginary part of propagation constant. which can be calculated by the Eq. 4.4 and Eq. 4.5.

The effective-mode-area (EMA) of the fundamental mode of structure can be determined by transverse electric field of mode using following relation given in Eq. 4.6 [78].

$$A_{eff} = \frac{(\iint |E|^2\, dx\, dy)^2}{(\iint |E|^4 dx\, dy)} \qquad (4.6)$$

4.4 Numerical Results and Discussion

In the proposed RC SMSP PCF, we have explored the effective-mode-index (EMI), confinement loss (CL), and effective-mode-area (EMA) making use of full-vectorial FEM (based software) with a PML. The refractive-index of fused silica has been taken as 1.444 at 1.55 µm.

	MODE LP_{01}					
	X			**Y**		
r_1 (µm)	**n_{eff}**	**Confinement loss (dB/m)**	**EMA (μm^2)**	**n_{eff}**	**Confinement loss (dB/m)**	**EMA (μm^2)**
0.700	1.438602	5.65796	73.12	1.438527	141.29359	97.88
0.750	1.438611	1.34436	66.45	1.438529	35.36594	77.59
0.800	1.438426	0.23823	54.35	1.438330	4.65454	58.13
0.850	1.438256	0.13765	48.78	1.438212	2.76456	50.77
0.900	1.438157	0.00509	43.27	1.438040	0.01988	43.38
0.950	1.437024	0.00023	41.99	1.430000	0.00876	41.68
1.000	1.437933	0.00003	38.19	1.437793	0.00026	38.48

Table 4.1: Variation of EMI (n_{eff}), CL, and EMA of fundamental mode with x-polarization and with y-polarization with r_1.

	MODE LP_{01}					
	X			**Y**		
r_2 (µm)	**n_{eff}**	**Confinement loss (dB/m)**	**EMA (μm^2)**	**n_{eff}**	**Confinement loss (dB/m)**	**EMA (μm^2)**
1.000	1.440090	0.00056	58.02	1.440078	0.00054	58.02
1.500	1.439385	0.00140	52.68	1.439317	0.00745	53.26
1.700	1.439062	0.00721	52.74	1.438982	0.05402	53.88
1.800	1.438885	0.02087	53.67	1.438801	0.21389	55.34
1.900	1.438700	0.11073	55.83	1.438607	1.85074	59.12
2.000	1.438502	0.94321	60.77	1.438413	26.66763	67.23
2.100	1.438499	1.07154	60.96	1.438409	29.33818	69.41

Table 4.2: Variation of EMI (n_{eff}), CL, and EMA of fundamental mode with x-polarization and with y-polarization with r_2.

	MODE LP_{01}					
	X			Y		
Pitch (µm)	n_{eff}	Confinement loss (dB/m)	EMA (μm^2)	n_{eff}	Confinement loss (dB/m)	EMA (μm^2)
4.200	1.434648	47.63563	55.08	1.434419	315.08703	73.90
4.500	1.436451	8.43004	56.77	1.436335	240.29980	89.23
5.000	1.438502	0.94321	60.77	1.438413	26.66763	67.23
5.500	1.439842	0.30978	77.80	1.439785	3.38096	83.50
6.000	1.440748	0.48613	98.89	1.440714	3.21638	105.17
7.000	1.441869	0.16256	153.57	1.441855	1.08181	160.84

Table 4.3: Variation of EMI (n_{eff}), CL, and EMA of fundamental mode with x-polarization and with y-polarization with pitch.

	MODE LP_{01}					
	X			Y		
Wavelength (µm)	n_{eff}	Confinement loss (dB/m)	EMA (μm^2)	n_{eff}	Confinement loss (dB/m)	EMA (μm^2)
1.300	1.442924	0.41778	55.16	1.442867	6.51358	59.04
1.350	1.442067	0.47632	56.12	1.442004	8.32366	60.57
1.400	1.441198	0.55289	57.16	1.441129	10.82488	62.28
1.450	1.440316	0.65188	58.27	1.440240	14.35530	64.19
1.500	1.439417	0.77929	59.47	1.439335	19.39984	66.35
1.550	1.438502	0.94321	60.77	1.438413	26.66763	67.23
1.600	1.437569	1.15446	62.18	1.437473	37.19681	71.72

Table 4.4: Variation of EMI (n_{eff}), CL, and EMA of fundamental mode with x-polarization and with y-polarization with wavelength.

4.4.1 Effect of structural parameters on Effective-Mode-Index:

As illustrated in Fig.4.2, initially we have chosen the structural parameters, r_2 = 2 µm, Λ = 5 µm, then we observed the effect of r_1 on EMI of fundamental mode with x-polarization (*i.e.* LP_{01}(X)) and fundamental mode with y-polarization (*i.e.* LP_{01}(Y)). The EMI of both x and y-polarizations decreases with increase in r_1. This is because of the increment in air-filling fraction of structure on increasing r_1. The significant decrease in the effective-index of LP_{01}(X) compared to LP_{01}(Y) gives increase in CL and EMA.

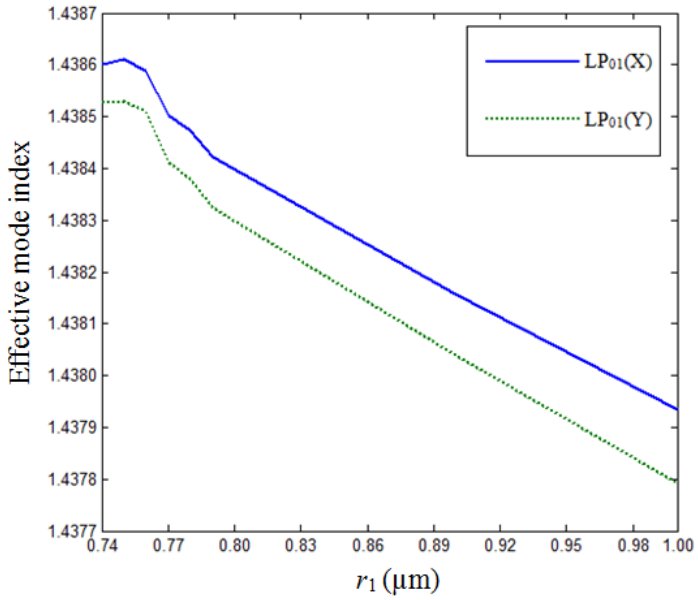

Fig.4.2: Variation of EMI of fundamental mode with x-polarization and with y-polarization with r_1.

In Fig.4.3, we have shown the effect of r_2 on EMI of fundamental mode ($LP_{01}(X)$ & $LP_{01}(Y)$). The EMI of fundamental mode with x-polarization and y-polarization is significantly decreased with increase in r_2. This happens because of the increase in the air-filling fraction in the cladding area of PCF.

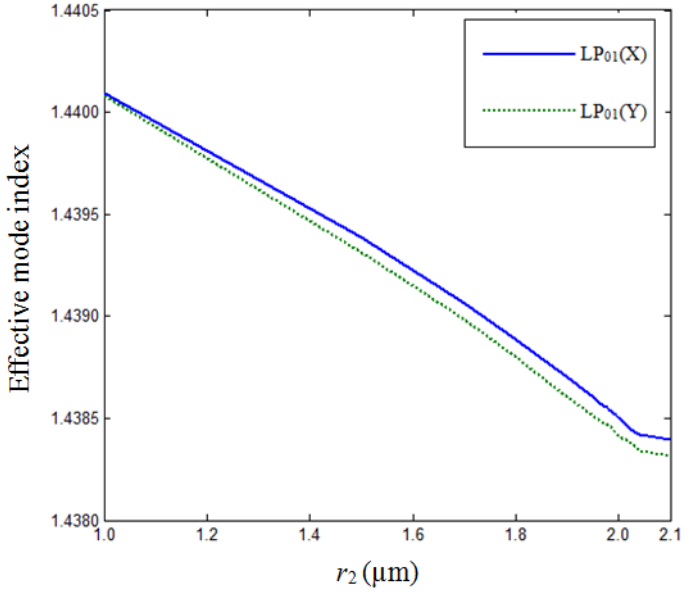

Fig.4.3: Variation of EMI of fundamental mode with x-polarization and with y-polarization with r_2.

Figure 4.4 indicates the variation of EMI of fundamental mode with x-polarization (*i.e.* $LP_{01}(X)$) and fundamental mode with y-polarization (*i.e.* $LP_{01}(Y)$) with pitch. The effective-mode-indices of the both polarizations increase with pitch. The air-filling fraction decreases on increasing the hole to hole distance which leads to increment in effective-mode-indices of modes.

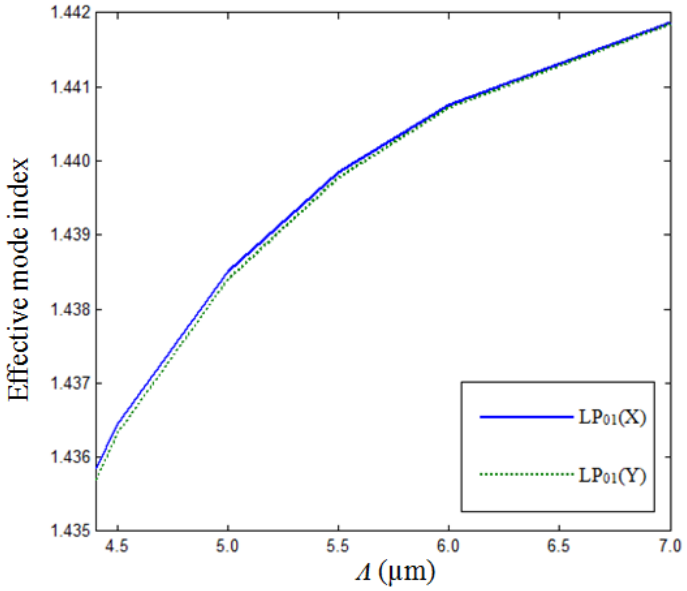

Fig. 4.4: Variation of EMI of fundamental mode with x-polarization and with y-polarization with pitch.

4.4.2 Effect of wavelength on Effective-Mode-Index:

Figure 4.5 indicates the variation of effective-mode-index of fundamental mode (*i.e.* $LP_{01}(X)$ & $LP_{01}(Y)$) with wavelength band between 1.30 - 1.60 μm. The EMI of both polarizations is decreases with increase in λ. This happens due to change in refractive-index of silica, the refractive-index is depending on wavelength.

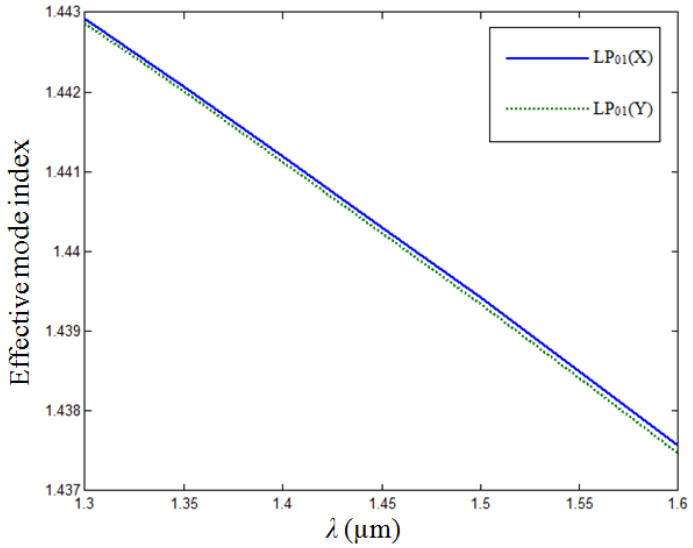

Fig.4.5: Variation of EMI of fundamental mode with x-polarization and with y-polarization with wavelength (*λ*).

4.4.3 Effect of structural parameters on Confinement Loss:

The following Fig.4.6, shows the variation of CLes of fundamental mode with x-polarization and y-polarization of proposed RC SPSM PCF structure. Initially, the CLes of both polarizations of fundamental mode are very high and then start to decrease on increasing r_1. Small peak is observed around r_1 = 0.77 μm this is due to the resonance effect of $LP_{01}(Y)$ mode to the cladding at this value of r_1. The resonance effect is high when r_1 = 0.77 μm with CL of 26.67 dB/m of y-polarization and 0.94 dB/m of x-polarization. At lower values of r_1, both polarizations have high losses. The CL of $LP_{01}(X)$ mode is very less as compare to $LP_{01}(Y)$ mode so $LP_{01}(Y)$ mode gets filter it out from the core region after small distance of the PCF.

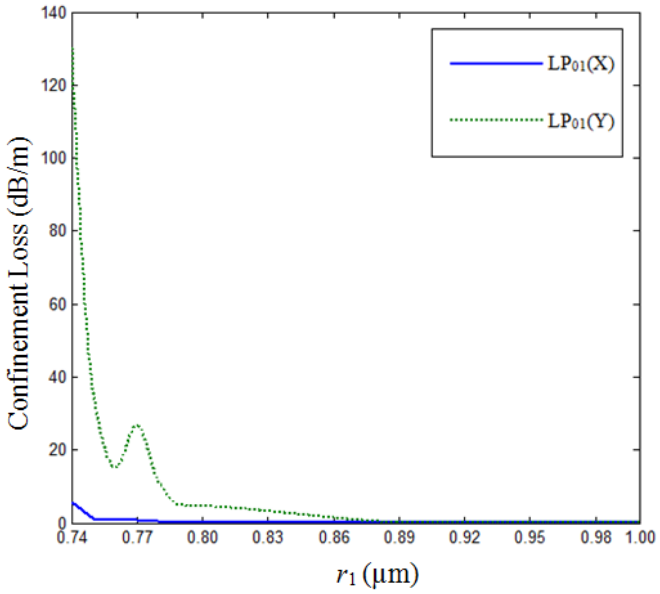

Fig.4.6: Variation of the CL of $LP_{01}(X)$ & $LP_{01}(Y)$ of fundamental mode with r_1.

The variation of CL of $LP_{01}(X)$ & $LP_{01}(Y)$ of fundamental mode on r_2 has been shown in Fig.4.7. The CL of $LP_{01}(X)$ mode is very less as compare to that of $LP_{01}(Y)$ mode. At r_2 = 2 µm the CL of $LP_{01}(X)$ mode is 0.94 dB/m and CL of $LP_{01}(Y)$ mode is around 26.67 dB/m. The CLes of both polarizations increase with r_2 due to decrease in the core size.

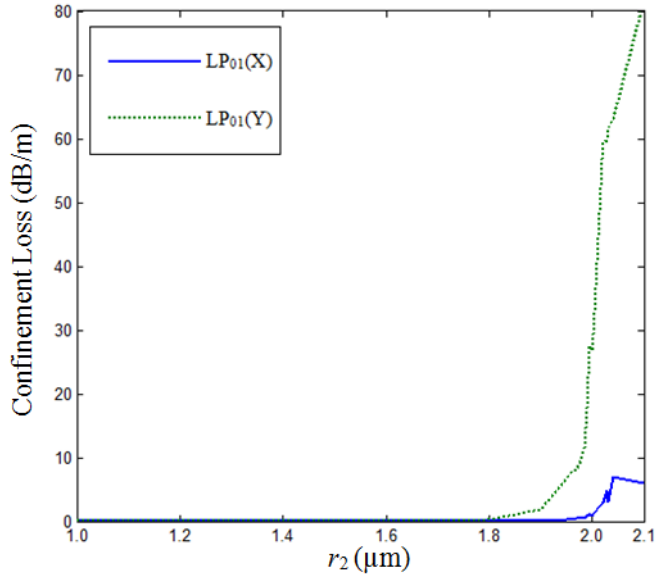

Fig.4.7: Variation of the CL of $LP_{01}(X)$ & $LP_{01}(Y)$ of fundamental mode with r_2.

The effect on CL of $LP_{01}(X)$ & $LP_{01}(Y)$ of fundamental mode of proposed RC SMSP PCF structure due to pitch has been investigated in Fig.4.8. The CL of $LP_{01}(X)$ mode is always very less as compare to $LP_{01}(Y)$ mode. There is significant decrement in the CL of $LP_{01}(Y)$

mode on increasing pitch. This is because of increase in size of core on increasing pitch. At Λ = 4.5 µm the CL of $LP_{01}(X)$ mode is 8.44 dB/m and $LP_{01}(Y)$ mode is 37.52 dB/m and at Λ = 5.5 µm the CL of $LP_{01}(X)$ mode is 0.34 dB/m and $LP_{01}(Y)$ mode is 3.38 dB/m. Thus we can state that the loss difference between the x as well as y-polarization is turns down as pitch increases.

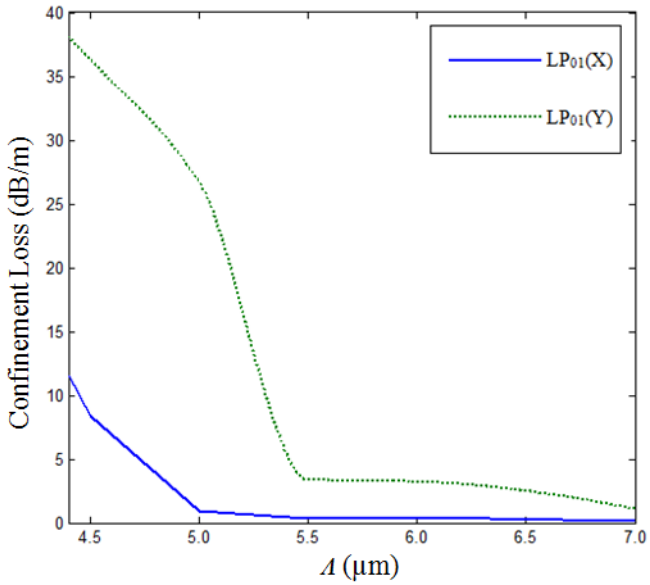

Fig.4.8: Variation of the CL of $LP_{01}(X)$ & $LP_{01}(Y)$ of fundamental mode with pitch.

4.4.4 Effect of wavelength on Confinement Loss:

The spectral dependence of the CL of $LP_{01}(X)$ & $LP_{01}(Y)$ of fundamental mode for proposed RC SPSM PCF structure has been exposed in Fig.4.9. The CL of $LP_{01}(X)$ mode is always less as compare to that of $LP_{01}(Y)$ mode within the spectral range of 1.3 - 1.6 µm. The CLes for both polarizations of the fundamental mode increase with wavelength. At 1.30 µm, the CL of $LP_{01}(X)$ mode is 0.42 dB/m and $LP_{01}(Y)$ mode is 6.51 dB/m. Therefore, after 3.07 m length of fiber the CL of $LP_{01}(Y)$ mode exceeds 20 dB while the CL of $LP_{01}(X)$ mode would only be 1.25 dB. Thus, SPSM operation is possible after 3.07 m length of PCF for wavelength of 1.3 µm. At 1.60 µm the CL of $LP_{01}(X)$ mode is 1.14 dB/m and $LP_{01}(Y)$ mode is 37.19 dB/m so after only 0.54 m length of the PCF the CL of $LP_{01}(Y)$ mode exceeds 20 dB while the CL of $LP_{01}(X)$ mode would only be 0.68 dB. For the wavelength of 1.6 µm, only 0.54 m long PCF structure is able to offers SPSM operation.

At 1.55 µm the CL of $LP_{01}(X)$ mode is 0.94 dB/m and $LP_{01}(Y)$ mode is 26.69 dB/m. So travelling to 0.75 m along the length of PCF the confinement loss of $LP_{01}(Y)$ mode exceeds

20 dB while the CL of $LP_{01}(X)$ mode would only be 0.70 dB. Therefore at 1.55 µm, only 0.70 m length of PCF is enough to achieve SPSM operation.

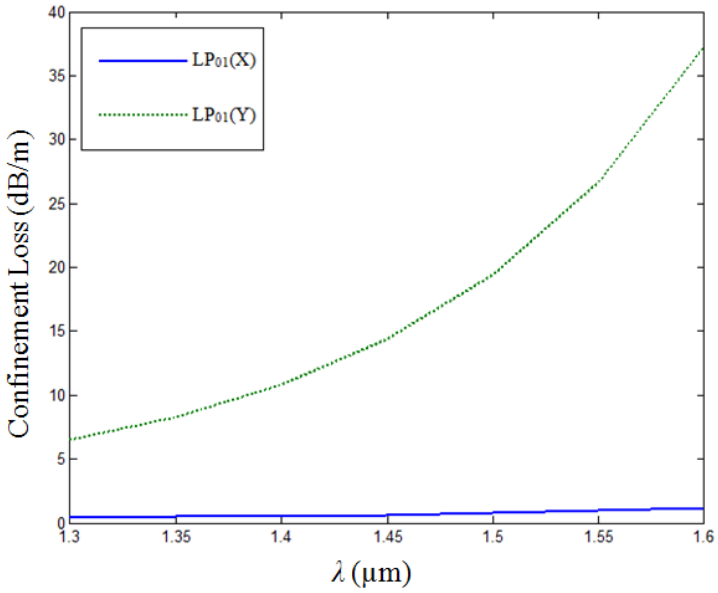

Fig.4.9: Variation of the confinement loss of $LP_{01}(X)$ & $LP_{01}(Y)$ of fundamental mode with wavelength.

4.4.5 Effect of structural parameters on Effective-Mode-Area:

Figure 4.10, illustrates the variation of EMA of x and y-polarization of fundamental mode with structural parameter r_1 of proposed RC SMSP PCF structure. The EMA decreases with r_1. At r_1 = 0.77 µm the EMA of x-polarized mode is 60.77 μm^2 and y-polarized mode is 67.23 μm^2.

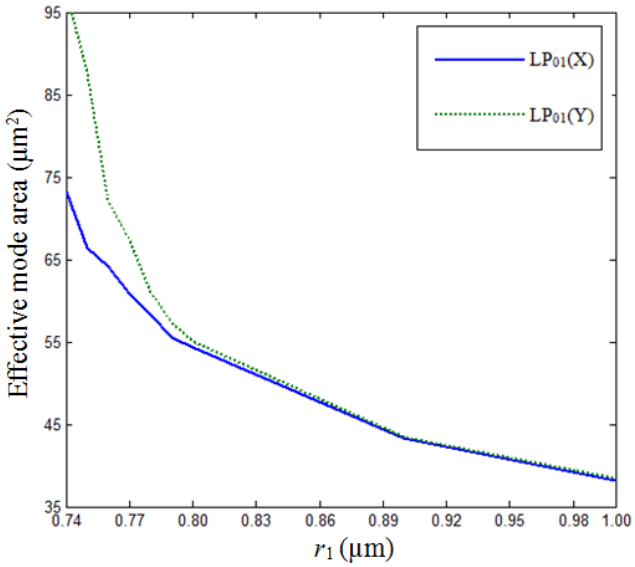

Fig.4.10: Variation of EMA of $LP_{01}(X)$ & $LP_{01}(Y)$ of fundamental mode with r_1.

In Fig.4.11, we have shown the effect of r_2 on EMA of x and y-polarization of fundamental mode. Initially, the EMA of x-polarized fundamental mode and y-polarized fundamental mode decreases with r_2, EMA of x-polarization is 60.67 μm^2 and y-polarization is 67.23 μm^2 around 2 μm and later EMA increases with r_2, it is due to the effect of increase in numerical aperture on increasing the size of air-holes in cladding region.

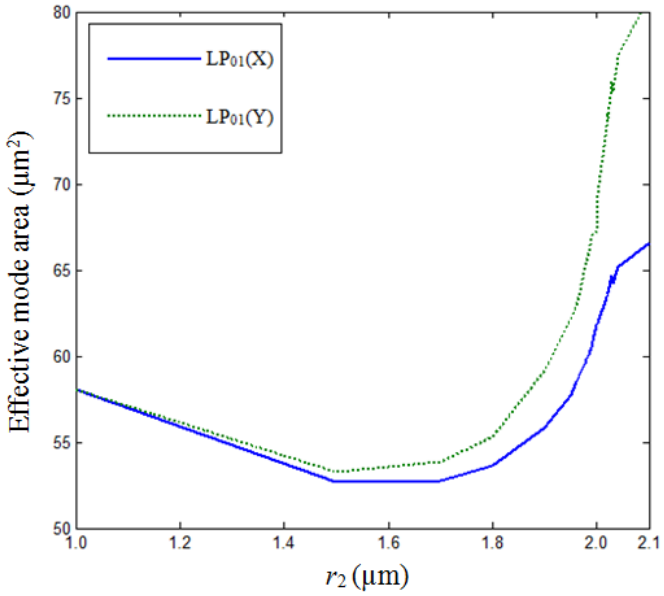

Fig.4.11: Variation of EMA of $LP_{01}(X)$ & $LP_{01}(Y)$ of fundamental mode with r_2.

EMA of x and y-polarization of fundamental mode of proposed RC SPSM PCF structure with pitch has been illustrated in Fig.4.12. This shows that EMA of fundamental mode with x-

polarization and y-polarization increases with pitch. This happens as the value of pitch increased then it leads to the increment in the core size. When pitch is 5 µm, the EMA of x-polarization is 60.67 μm^2 and y-polarization is 67.23 μm^2.

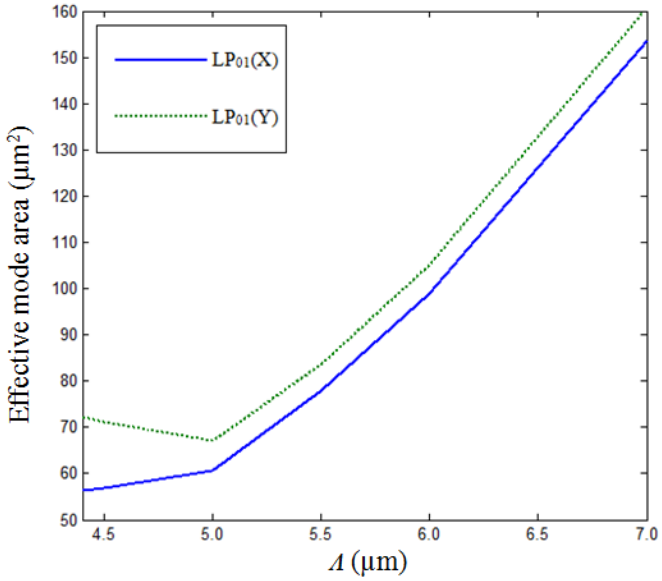

Fig.4.12: Variation of EMA of $LP_{01}(X)$ & $LP_{01}(Y)$ of fundamental mode with pitch.

4.4.6 Effect of wavelength on Effective-Mode-Area:

Figure 4.13 depicts the dependence of EMA of x and y-polarization of fundamental mode on values of wavelength. EMA of both polarizations increases with wavelength. At 1.30 µm wavelength, the confinement loss and EMA is obtained as 0.41 dB/m and 55.14 μm^2 for x-polarization as well as 6.51 dB/m and 59.03 μm^2 for y-polarization of fundamental mode respectively.

At 1.6 µm the confinement loss and EMA is obtained as 1.15 dB/m and 62.18 μm^2 for x-polarization as well as 37.19dB/m and 71.72 μm^2 for y-polarization of fundamental mode respectively.

The birefringence leads to the difference between the loss of x-polarization and y-polarization is very high, which indicates the single polarization single mode operation in this wavelength range. SMSP PCF with significantly high EMA is possible within the spectral range of 1.3 – 1.6 µm.

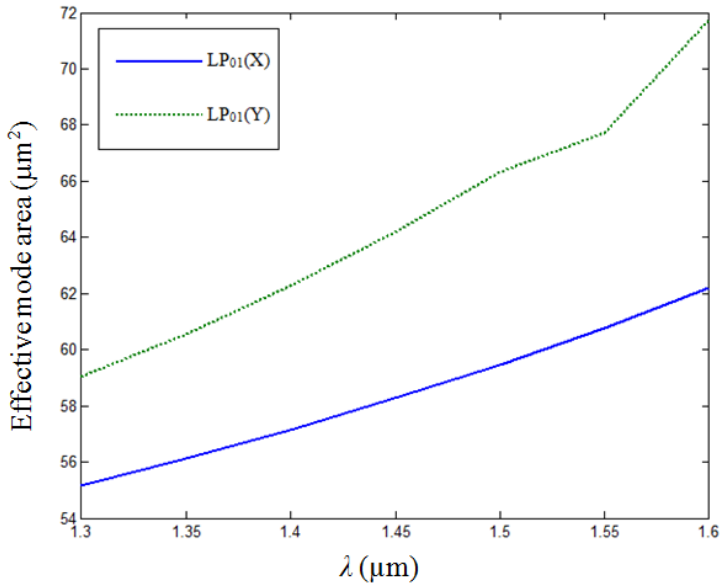

Fig.4.13: Variation of EMA of of $LP_{01}(X)$ & $LP_{01}(Y)$ of fundamental mode with wavelength.

At the end, the contour plots of x and y-polarization of the fundamental mode have been shown in Fig.4.14 at wavelength, λ= 1.55 μm, r_1 = 0.77 μm, r_2 = 2 μm, and Λ = 5 μm. It can be observed from figure that $LP_{01}(X)$ mode is well confined within the core while $LP_{01}(Y)$ mode is leaking out from the core.

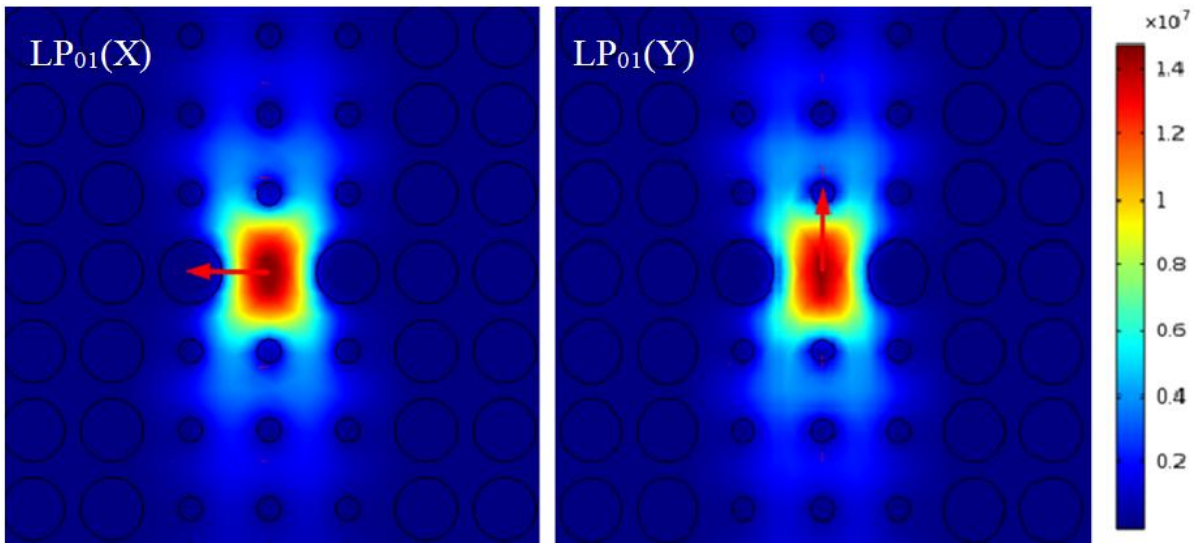

Fig.4.14: Contour plot of field intensity of $LP_{01}(X)$ & $LP_{01}(Y)$ modes at optimized parameters.

Chapter 5

CONCLUSION AND SCOPE FOR FUTURE WORK

5.1 Conclusion:

Rectangular-core photonic crystal fiber structure has been designed and analyzed for single-mode single-polarization operation with help of software which is using full vector finite-element-method. By choosing proper structural parameter we can tune the confinement loss of x and y-polarized fundamental mode of proposed rectangular-core single-mode single-polarization photonic crystal fiber structure. The proposed photonic crystal structure offers the single-mode single-polarization operation within the spectral or wavelength range of 1.3-1.6 µm. At 1.55 µm, the proposed structure possesses the confinement loss of 0.95 dB/m and effective-mode-area as high as 60.67 μm^2 for x-polarization of fundamental mode while the confinement loss of 26.67 dB/m and effective-mode-area of as high as 67.24 μm^2 for y-polarization of fundamental mode. The confinement loss of $LP_{01}(x)$ mode is very low which is the propagating mode and the confinement loss of $LP_{01}(y)$ is sufficiently high to leak it out from the core of proposed rectangular-core single-mode single-polarization photonic crystal fiber structure. Simulation results shows that, after travelling approximately 0.75 m distance through photonic crystal fiber the LP_{01} (y) mode offers more than 20 dB loss on the other hand $LP_{01}(x)$ mode offers only 0.70 dB loss. Therefore, proposed photonic crystal fiber structure offers effective single-polarization single-mode operation after 0.75 m distance of proposed photonic crystal fiber with effective-mode-area as high as 60.67 μm^2. Such PCF structure has potential applications in area of compact optical devices and high power optical communication systems.

5.2 Scope for Future Work:

Birefringence: The birefringence of fundamental mode need to increase more and more for various applications in the field of optical polarizer.

Nonlinear applications: For nonlinear applications fiber needed to be polarized as well as with very low effective mode area for most applications in field of optical sensors.

Large-mode-area: PCF is now finding various applications in optical-fiber communications, low/high power optical amplifiers, low/high power fiber lasers, non-linear devices, high

power transmission, gas sensors, and other exciting areas. As day by day power requirements are increasing, lots of improvements are needed, in increasing confinement loss of higher order modes for single-mode operation and effective-mode-area of the fundamental mode for large power operations. These designed photonic crystal fibers changes its properties when they are bent, so bending performance is also need to check.

REFERENCES

1. Optical Fiber Communications by G. Keiser.
2. Optical Fiber Communications by J.M. Senior, M.Y. Jamro.
3. P.S.J. Russell, R. Dettmer, "A neat idea [Photonic crystal fiber]", IEE Review 47, 19-23 (2001).
4. P.S.J. Russell, "Photonic crystal fiber", Science 229, 358-362 (2003).
5. J.C. Knight, T.A. Birks, P.S.J. Russell, D.M. Atkin, "All-silica single-mode optical fiber with photonic crystal cladding," Opt. Lett. 21, 1547-1549 (1996).
6. J.C. Knight, "Review article photonic crystal fibers" Nature 424, 847-851(2003).
7. J.C. Knight, T.A. Birks, P.S.J. Russell, "Photonic band cap guidance in optical fibers," Science 282, 1476-1478 (1998).
8. R.F. Cregan, B.J. Mangan, J.C. Knight, T.A. Birks, P.S.J. Russell, P.J. Roberts, D.C. Allan, "Single-mode photonic band gap guidance of light in air," Science 285, no. 5433,1537–1539, (1999).
9. K. Kiang, K. Frampton, T. Monro, R. Moore, J. Tucknott, D. Hevak, N. Broderick, D. Richardson, H. Rutt, "Extruded single mode non-silica glass holey optical fibres," Electron. Letts. vol. 38, 546-547 (2002)
10. J.S.A. Cerqueira, "Recent progress and novel applications of photonic crystal fibers", Rep. Prog. Phys. 73 (2010)
11. J. Dia, J.A. Harrington, "High-peak-power, Pulsed CO2 laser light delivery by hollow glass waveguides", Appl. Opt. 36, 5072-5077 (1997)
12. M.N. Petrovich, F. Poletti, A. Van Barkel, D.J. Richardson, "Robustly single mode hollow core photonic bandgap fiber ", Opt. express 16, 4337-4346 (2008)
13. P. Roberts, F. Couny, H. Sabert, B. Mangan, D. Williams, L. Farr, M. Mason, A. Tomlinson, T.A. Birks, J.C. Knight, P.S.J. Russell, "Ultimate low loss of hollow-core photonic crystal fibres" Opt. Express 13, 236–244 (2005).
14. F. Luan, A.K. George, T.D. Headdley, D.M. Bird, J.C. Knight, P.S.J. Russell, "All solid bandgap fiber", Opt. Lett. 29, 1-4 (2004)
15. A. Argyros, T.A. Briks, S.G. Leon-Saval, C.M.B. Cordeiro, F. Luan, P.S.J. Russell, "Photonic Band gap with an index step of one percent", Opt. Express 13, 1540-1550 (2004)

16. S.J.A. Cerqueira, F. Luan, C.M.B. Cordeiro, A.K. George, J.C. Knight, "Hybrid photonic crystal fiber", Opt. Express 14, 926–931(2006).
17. T.A. Birks, J.C. Knight, P.S.J. Russell, "Endlessly single-mode photonic crystal fiber" Opt. Lett. 22 , 961 (1997).
18. J.C. Knight, T.A. Birks, P.S.J. Russell, J.P. de Sandro, "Properties of photonic crystal fiber and the effective index model," J. Opt. Soc. Am. A 15, 748-752 (1998).
19. J.C. Baggett, T.M. Monro, K. Furusawa, D.J. Richardson, "Comparative study of large mode holey and conventional fibers," Opt. Lett. 26, 1045-1047 (2001).
20. L. Xin, Z. Hong-Jun, W. Chong-Qing, L. Shan-Liang, "A novel single polarization single mode photonic crystal fiber with circular and elliptical air holes arrays", Optoelectronics let. 9, 120-123 (2013).
21. A. Ferrando, E. Silvestre, P. Andres, J.J. Miret, M.V. Andres, "Designing the properties of dispersion-flattened photonic crystal fibers," Opt. Express 9, 678 (2001).
22. T.M. Monro, Y.D. West, D.W. Hewak, N.G.R. Broderick, D.J. Richardson, "Chalcogenide holey fibres," Electron. Lett. 36, 1998-2000 (2000).
23. J.Y.Y. Leong, et al, "Highly-nonlinearity dispersion shifted lead silicate holey fibers for efficient 1 µm pumped supercontinuum generation", J. Lightwave Technology 24, 183(2006).
24. H. Ebendroff-Heidepriem, P. Petropoulos, S. Asimakis, V. Fainazzi, R.C. Moore, K. Frampton, F. Koizumo, D.J. Richardson, T.M. Monro, "Bismuth glass holey fibers with high nonlinearity", Opti. Express 12, 5082-5087 (2004)
25. V.V. Ravi Kanth Kumar, A.K. George, W.H. Reeves, J.C. Knight, P.S.J. Russell, "Extruded soft glass photonic crystal fiber for ultra board supercontinuum generation" Opt. Express 10, 1520-1525 (2002).
26. M.A.V. Eijkelenborg et al "Microstructured polymer optical fiber" Opt. Express 9, 319–327 (2001)
27. A. Ferrando, E. Silvester, J. J. Miret, P. Andres, M.V. Andres, "Full vector analysis of a realistic photonic crystal fiber," Opt. Lett., vol. 24,no. 5, 276–278, (1999).
28. A. Ferrando, E. Silvestre, J.J. Miret, P. Andres, "Vector description of higher-order modes in photonic crystal fibers," J. Opt. Soc. Amer. A, vol. 17, no. 7, 1333–1340, (2000).
29. S.E. Barkou, J. Broeng, A. Bjarklev, "Silica-air photonic crystal fiber design that permits wave guiding by a true photonic bandgap effect," Opt. Lett., vol. 24, no. 1, 46–48, (1999).

30. J. Broeng, S.E. Barkou, T. Sondergaard, A. Bjarklev, "Analysis of air-guiding photonic bandgap fibers," Opt. Lett., vol. 25, no. 2, 96–98 (2000).
31. D. Mogilevtsev, T.A. Birks, P. S. J. Russell, "Localized function method for modeling defect modes in 2-D photonic crystals," J. Lightw.Technol., vol. 17, no. 11, 2078–2081, (1999).
32. T.M. Monro, D.J. Richardson, N.G.R. Broderick, P.J. Bennett, "Modeling large air fraction holey optical fibers," J. Lightw. Technol., vol. 18, no. 1, 50–56,(2000).
33. T.P. White, R.C. McPhedran, L.C. Botten, G.H. Smith, C.M. de Sterke, " Calculations of air-guided modes in photonic crystal fibers using the multipole method" Opt. Express [Online].9(13), 721–732. (2001).
34. T.P. White, B.T. Kuhlmey, R.C. McPhedran, D. Maystre, G. Renversez, C.M. de Sterke, L.C. Botten, "Multipole method for microstructured optical fibers. I. Formulation", J. Opt. Soc. Amer. B, vol. 19, no. 10, 2322–2330, (2002).
35. B.T. Kuhlmey, T.P. White, G. Renversez, D. Maystre, L.C. Botten, C.M. de Sterke, R.C. McPhedran, "Multipole method for microstructured optical fibers. II. Implementation and results", J. Opt. Soc. Amer. B, vol. 19, no. 10, 2331–2340, (2002).
36. C.E. Kerbage, B.J. Eggleton, P.S. Westbrook, R.S. Windeler, "Experimental and scalar beam propagation analysis of an air-silica microstructure fiber", Opt. Express [Online]. 7(3), 113–122. (2000).
37. B.J. Eggleton, P.S. Westbrook, C.A. White, C. Kerbage, R.S. Windeler, G.L. Burdge, "Cladding-mode resonances in air-silica microstructure optical fibers," J. Lightw. Technol., vol. 18, no. 8, 1084–1100, (2000).
38. F. Fogli, L. Saccomandi, and P. Bassi, "Full vectorial BPM modeling of index-guiding photonic crystal fibers and couplers", Opt. Express [Online]. 10(1), 54–59. (2002).
39. Z. Zhu and T.G. Brown, "Full-vectorial finite-difference analysis of microstructured optical fibers", Opt. Express [Online]. 10(17), 853–864 (2002).
40. G.E. Town and J.T. Lizer, "Tapered holey fibers for spot-size and numerical-aperture conversion," Opt. Lett., vol. 26, no. 14, 1042–1044 (2001).
41. J.T. Lizier and G.E. Town, "Splice losses in holey optical fibers," IEEE Photon. Technol. Lett., vol. 13, no. 8, 794–796 (2001).
42. M. Qiu, "Analysis of guided modes in photonic crystal fibers using the finite-difference time-domain method," Microw. Opt. Technol. Lett.,vol. 30, no. 5, 327–330 (2001).

43. N. Guan, S. Habu, K. Takenaga, K. Himeno, A. Wada, "Boundary element method for analysis of holey optical fibers," J. Lightw. Technol.vol. 21, no. 8, 1787–1792 (2003).
44. T.L. Wu, C.H. Chao, "Photonic crystal fiber analysis through the vector boundary-element method: Effect of elliptical air hole," IEEE Photon.Technol. Lett., vol. 16, no. 1, 126–128, (2004).
45. A. Ferrando, E. Silvestre, J.J. Miret, P. Andres, M.V. Andres, "Full-vector analysis of a realistic photonic crystal fiber" Opt. Lett. 24, 276 (1999).
46. S. Cucinotta, S. Selleri, L. Vincetti, and M. Zoboli, "Holey fiber analysis through the finite element method," IEEE Photon. Technol. Lett. 14, 1530-1532 (2002).
47. J.C. Knight and P.S.J. Russell, "Photonic crystal fibers: New way to guide light," Science, vol. 296, no. 5566, 276–277, (2002).
48. W.H. Reeves, D.V. Skryabin, F. Biancalana, J.C. Knight, P.S. J. Russell, F.G. Omenetto, A. Efimov, A.J. Taylor, "Transformation and control of ultra-short pulses in dispersion-engineered photonic crystal fibers", Nature 424, 511(2003) .
49. J. Wang, C. Jiang, W. Hu, M. Gao, "Modified design of photonic crystal fibers with flattened dispersion", Optics & Laser Tech. 38 (3) 169-172 (2006).
50. P. Morin, B. Kibler, J. Fatome, C. Finot, G. Millot, "Group modal birefringence inversion in a highly birefringent nonlinear photonic crystal fibre at telecommunication wavelengths", Electronics Letters/IEE Electronics Letters 46 (7) 525-526 (2010).
51. J. Liao, J. Sun, "High birefringent rectangular-lattice photonic crystal fibers with low confinement loss employing different sizes of elliptical air holes in the cladding and the core", Opt. Fiber Tech 18 (6), 457–461 (2012).
52. I. Abdelaziz, H. Ademgil, F. AbdelMalek, S. Haxha, T. Gorman, H. Bouchriha, "Design of a large effective- mode-area photonic crystal fiber with modified rings", Opt. Comm. 283, 5218-5223 (2010).
53. K. Kishor, R.K. Sinha, A.D. Varshney, "Experimental verification of improved effective index method for endlessly single mode photonic crystal fiber", Optics and Lasers in Engineering 50, 182-186 (2012).
54. T.S. Saini, A. Kumar, R.K. Sinha, "Triangular-core large-mode-area photonic crystal fiber with low bending loss for high power applications," Appl. Opt. 53 (31), 7246 – 4251 (2014).
55. T.S. Saini, A. Kumar, R.K. Sinha, "Broadband mid-IR supercontinuum generation in As2Se3 based chalcogenide photonic crystal fiber: A new design and analysis," Opt. Commun. 347, 13 – 19 (2015).

56. J.M. Dudley, "Supercontinuum generation in photonic crystal fiber", Rev. Mod. Phys., 78, 4 (2006).
57. X. Dong, H. Tam, P. Shum, "Temperature-insensitive strain sensor with polarization-maintaining photonic crystal fiber based Sagnac interferometer," Appl. Phys. Lett. 90, 151113 (2007).
58. J.R. Simpson, R.H. Stolen, F.M. Sears, W. Pleibel, J.B. Macchesney, R. E. Howard, "A single-polarization fiber," J. Lightw. Technol., vol. LT-1, no. 2, pp. 370–373, (1983).
59. M.J. Messerly, J.R. Onstott, R.C. Mikkelson, "A broad-band single polarization optical fiber," J. Lightw. Technol., vol. 9, no. 7, pp. 817–820, (1991).
60. K. Okamoto, "Single-polarization operation in highly birefringent optical fibers," Appl. Opt., vol. 23, no. 15, 2638–2642, (1984).
61. A. Ortigosa-Blanch, J.C. Knight, W.J. Wadsworth, J. Arriaga, B. J.Mangan, T.A. Birks, P.S.J. Russell, "Highly birefringent photonic crystal fibers," Opt. Lett., vol. 25, no. 18, 1325–1327, (2000).
62. K. Suzuki, H. Kubota, S. Kawanishi, M. Tanaka, M. Fujita, "High speed bi-directional polarization division multiplexed optical transmission in ultra low-loss (1.3 dB/km) polarization-maintaining photonic crystal fiber," Electron. Lett., vol. 37, no. 23, 1399–1401, (2001).
63. P. Pual, "Optical properties of a low-loss polarization-maintaining photonic crystal fiber," Opt. Express, vol. 9, no. 13, 676–680, (2001).
64. T.P. Hansen, J. Broeng, S.E.B. Libori, E. Knuders, A. Bjarklev, J.R. Jensen, H. Simonsen, "Highly birefringent index-guiding photonic crystal fibers," IEEE Photon. Technol. Lett., vol. 13, no. 6, 588–590, (2001).
65. K. Saitoh, M. Koshiba, "Photonic bandgap fibers with high birefringence," IEEE Photon. Technol. Lett., vol. 14, no. 9, 1291–1293, (2002).
66. P.R. Chaudhuri, V. Paulose, C. Zhao, C. Lu, "Near-elliptic core polarization-maintaining photonic crystal fiber: Modeling birefringence characteristics and realization," IEEE Photon. Technol. Lett., vol. 16, no. 5, 1301–1303, (2004).
67. K. Saitoh, M. Koshiba, "Single-polarization single-mode photonic crystal fibers," IEEE Photon. Technol. Lett., vol. 15, no. 10, 1384–1386, (2003).
68. H. Kubota, S. Kawanishi, S. Koyanagi, M. Tanaka, and S. Yamaguchi, "Absolutely single polarization photonic crystal fiber," IEEE Photon. Technol. Lett., vol. 16, no. 1, 182–184, (2004).
69. M. Li, "High bandwidth single polarization fiber with elliptical central air hole," J. Lightwave Technology, 23, 3454-3460 (2005).

70. T. Schreiber, F. Roser, O. Schmidt, J. Limpert, R. Iliew, F. Lederer, A. Petersson, C. Jacobsen, K. P. Hansen, J. Broeng, A. Tunnermann, "Stress-induced single-polarization single-transverse mode photonic crystal fiber with low nonlinearity," Opt. Express, 13, 7621-7630 (2005).
71. X. Chen, M.J. Li, J. Koh , D.A. Nolan., "Wide band single polarization and polarization maintaining fibers using stress rods and air holes," Opt. Express, 16, 12060-12068 (2008).
72. F. Zhang, M. Zhang , X Liu ,Ye, Peida, "Design of wideband single-polarization single-mode photonic crystal fiber," J. Lightw. Technol.,25, 1184-1189 (2007).
73. C. Xiong and W.J. Wadsworth, "Polarized supercontinuum in birefringent photonic crystal fibre pumped at 1064 nm and application to tunable visible/UV generation," Opt. Express, 16, 2438-2445 (2008).
74. J. Ju, W. Jin, M.S. Demokan, "Design of single-polarization Photonic crystal fiber at 1.30 and 1.55 um" J. Lightwave Technology, 24, 825-830. (2006).
75. I.H. Malitson, "Interspecimen comparison of the refractive index of fused silica", J. Opt. Soc. Am. 55 (10), 1205 (1965).
76. G.P. Agrawal, Fiber-optic Communication Systems (3rd Ed.), New York: John Wiley & Sons, Inc, (2002).
77. S. Haxha, H. Ademgil, "Novel design of photonic crystal fibers with low confinement losses near zero ultra-flatted chromatic dispersion, negative chromatic dispersion and improved effective mode area", Opt. Comm. 281, 278-86 (2008).
78. T.S. Saini, A. Kumar, V. Rastogi, R.K. Sinha "Selectively filled large-mode-area photonic crystal fiber for high power applications", Proceeding of SPIE Optics + Photonics 2013, USA, Vol. 8847, No. 61 (2013).

NOTES

NOTES